The Design of a Multi-Chip SMT Front-End Module for the 26 GHz 5G Pioneer Band

By by Graham Pearson*, Liam Devlin* and Mike Geent *Plextek RFI Ltd, ‡Filtronic Broadband Ltd

5G communications systems will offer huge increases in data rates and aim to provide a service with seemingly infinite capacity. This will be facilitated by the use of mm-wave frequencies, where large bands of contiguous spectrum can be made available. Although the mm-wave bands for 5G have yet to be confirmed, development work is already under way in several of the candidate bands, including the band around 26 GHz band that has been identified by the EU's Radio Spectrum Policy Group (RSPG) as the 'Pioneer Band' for 5G in Europe.

FREQUENCY BANDS

The agreement of the mm-wave bands for 5G will be finalised at the World Radio Conference in 2019 (WRC-19). The candidate bands [1] where development work is already taking place include the FCC licensed bands at 28 GHz (27.5 – 28.35 GHz), 37 GHz (37 – 38.6 GHz) and 39 GHz (38.6 – 40 GHz) and the 26 GHz European pioneer band (24.25 to 27.5 GHz).

The RSPG recommended the 26 GHz band as the pioneer band for mm-wave 5G in its Strategic Roadmap Towards Europe, published in November 2016 [2]. Those attempting to develop mm-wave equipment covering the 24.25 to 27.5 GHz band have discovered that component availability is somewhat limited.

This article describes the design, implementation and measured performance of an SMT packaged multi-chip front-end component intended to address this limitation. It comprises a low-noise amplifier (LNA), power amplifier (PA) and transmit/receive switch housed in a custom laminate surface mount (SMT) package measuring 10-mm x 10-mm. Low loss RF filtering has also been integrated into the package structure.

DESIGN AND IMPLEMENTATION

A single SMT component has been developed, which includes the mm-wave blocks of a Front-End Module (FEM) to cover the full 26 GHz 5G band (24.25 to 27.5 GHz). A block diagram depicting the functionality of the FEM is shown in Figure 1. It includes three GaAs MMICs

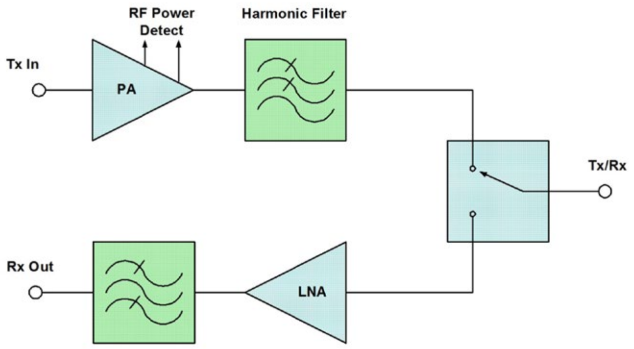

Figure 1: Block diagram of the 26 GHz FEM.

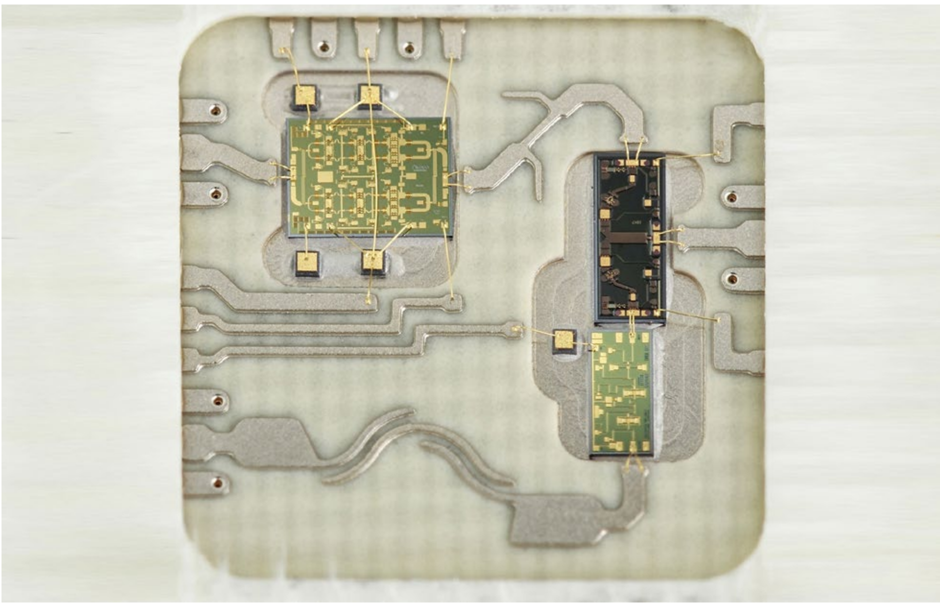

Figure 2: Photograph of the 26 GHz FEM prior to lidding.

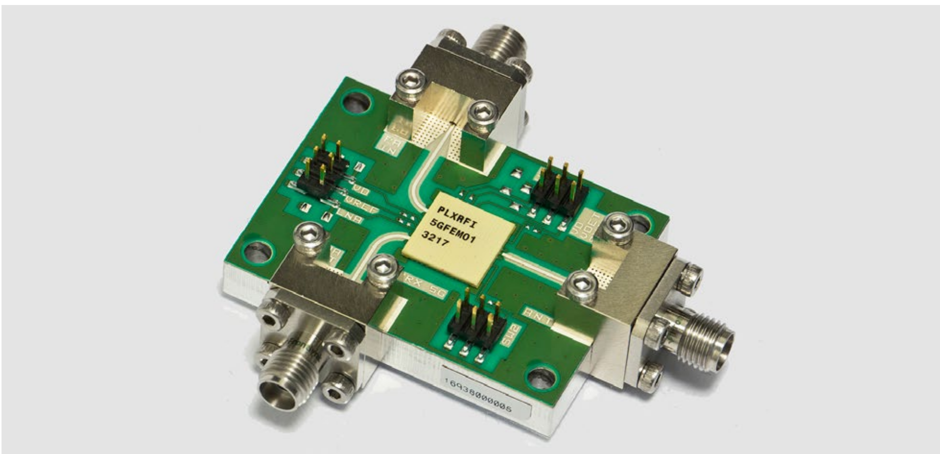

Figure 3: Photograph of the evaluation PCB with SMT FEM solder attached.

(LNA, PA and Tx/Rx switch) and two filters (low-pass filter after the PA for harmonic rejection and bandpass filter after the LNA).

The FEM is realised as a custom laminate package suitable for SMT assembly. A photograph of one of the assembled FEMs, prior to lidding, is shown in Figure 2. The three MMICs (PA, LNA and switch) are assembled into pockets in the laminate substrate material that forms the package. The backside of the ICs therefore sit on the metal base of the package, providing a good thermal contact to the PCB on which the FEM is ultimately mounted, and a low inductance interconnect to the PCB ground. It also means that the surface of the die is approximately level with the laminate surface inside the package, thus minimizing RF bond wire lengths and associated parasitics.

An advantage of the custom laminate package approach is the ability to integrate filters within the package structure, which helps to reduce both the size and cost of the FEM component. Such filters have been integrated into both the receive path (bandpass filter after the LNA) and the transmit path (low pass filter after the PA).

The PA die can be seen in the top left of Figure 2, followed by the integrated low-pass filter. This was designed to have a very low pass-band loss (around 0.2 dB) and to provide good harmonic rejection (in excess of 20 dB). The PA includes on-chip power detection that can be used to monitor the RF power transmitted by the FEM. The Tx/Rx switch at the common port of the FEM, on the right side, is a PIN diode MMIC, which is a technology that is well suited to the realisation of low-loss, high linearity mm-wave switches [3].

The LNA die is in the bottom right of the module, with the RF path moving from top to bottom of the die in the Y-direction. The band pass filter after the LNA is clearly visible as a coupled line structure. The coupled sections have been designed as curves rather than straight lines to allow for a more compact implementation. The shaped tracks at the input and output of the coupled line structure are part of the filter, and are critical in ensuring optimum performance.

The RF ports of the FEM package were carefully designed for optimum RF performance of the transition from the PCB, on which the component will be mounted, to the internal short 50Ω routing lines within the package. The parasitics of the PCB pads on the motherboard

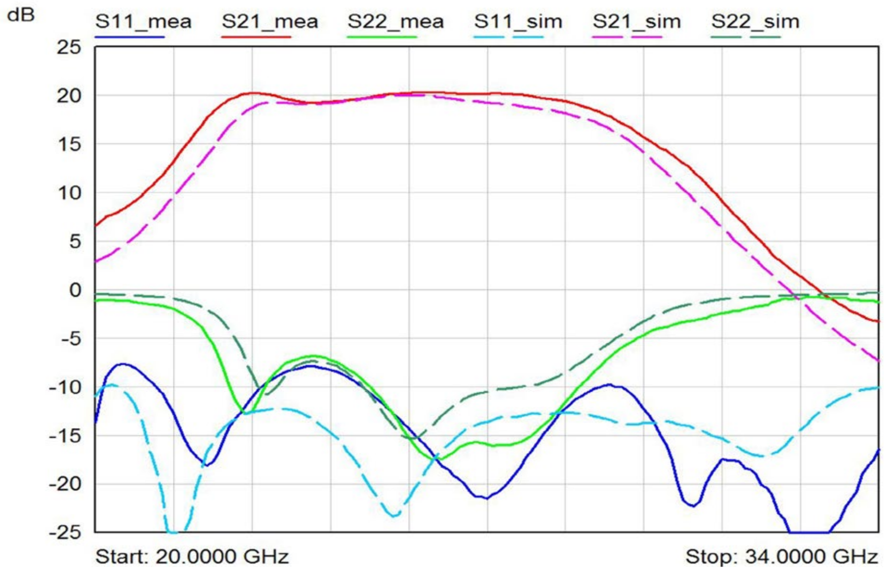

Figure 4: Measured receive path small-signal performance compared to simulated.

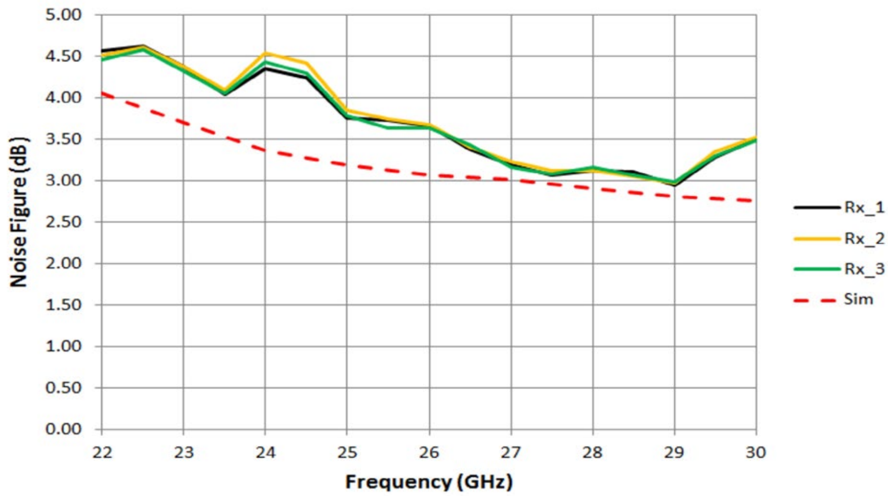

Figure 5: Measured receive path NF of 3 units compared to simulated.

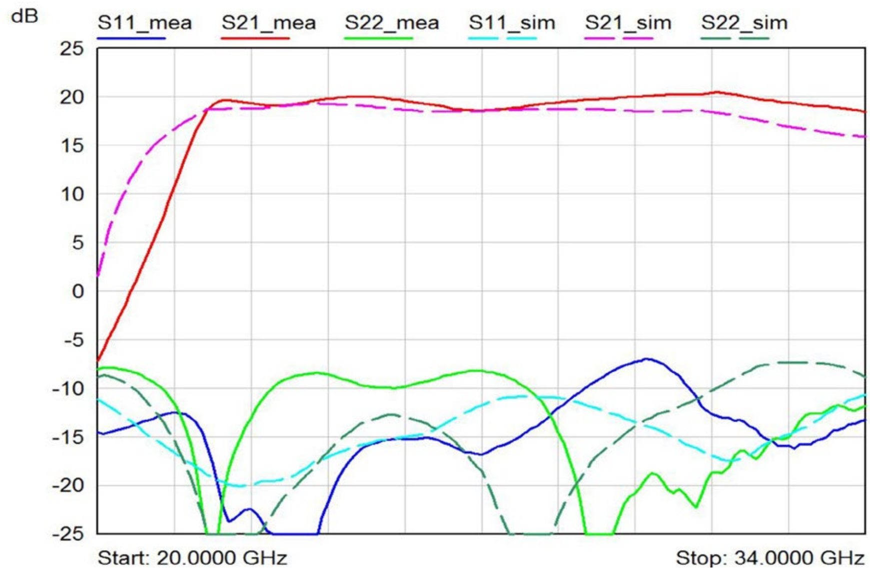

Figure 6: Measured transmit path small-signal performance compared to simulated.

and the vertical transitions through the laminate package were accounted for using EM simulation, and the overall structure was optimised to compensate for the parasitics and to ensure a good RF transition.

The RF interface to all MMICs within the package was also EM simulated and compensated to ensure optimum performance for the packaged MMIC. The short bond wire lengths and 'V' structure of the RF bonds to each MMIC are evident from the photograph. This helps to minimise the parasitic inductance of the RF bond connections and eases the process of optimising the RF performance of the whole FEM.

An evaluation PCB was designed on a low-cost laminate material, suitable for the realisation of high-volume mm-wave modules. The FEM components were assembled onto the evaluation PCB, which was attached to an aluminium carrier to provide ease of handling. A photograph of the evaluation PCB is shown in Figure 3. The base of the FEM is attached to an array of vias on the evaluation PCB to ensure a low inductance ground contact. Edge mounted mm-wave connectors are used to interface to all RF ports. Three 6-way SMT connectors were used for applying control and bias voltages to the FEM.

MEASURED PERFORMANCE

The performance of the FEM was measured on the evaluation PCB with the reference ports set at the package. TRL calibration structures realised on the same PCB material were used to facilitate this. The small signal measured performance of a typical receive path is plotted against frequency in Figure 4 along with the simulated performance (dotted traces). The band-pass shape of the gain response is predominantly defined by the bandpass filter. The receive amplifier (LNA) itself has a much broader band response.

It can be seen that the measured gain response is in close agreement with the simulated response, demonstrating the accuracy of the filter performance predicted in the EM simulations used to design the filter, and confirming the low loss of the bandpass filter integrated into the package.

The measured NF of three receive paths is plotted against frequency, along with the simulated (dashed red trace) in Figure 5. The mid-band NF is 3.6 dB, dropping to 3.1 dB at the top of the band and rising slightly at the lower end of the band. The switch loss is low (around 0.8 dB) and relatively constant across the band; the NF response is dominated by the LNA.

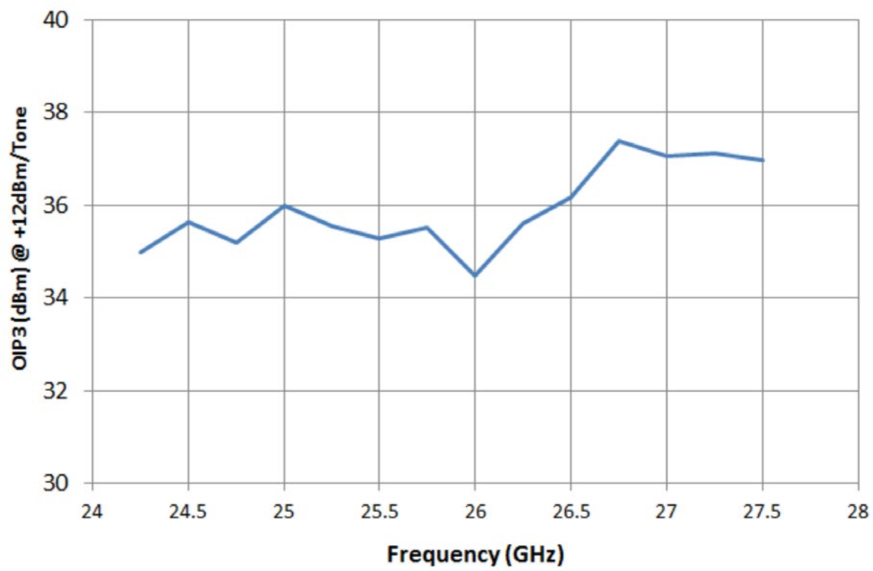

Figure 7: Measured transmit OIP3 versus frequency.

Figure 6 shows the measured small-signal performance of the transmit path versus frequency together with the simulated (dashed traces). As with the receive path, there is good agreement between simulated and measured performance. The harmonic filter starts to roll off significantly above 40 GHz (providing around 20 dB of rejection at the 2nd harmonic) and so its rejection performance is not evident in this plot. The close agreement between the in-band measured and simulated gains does, however, confirm the low insertion loss of the harmonic filter as predicted by the EM simulations used in the design process.

The linearity of the transmit chain was evaluated by measurement of the output-referred third order intercept point (OIP3). This measurement was made with the level of the two intermodulating tones set to +12 dBm at the common port of the FEM. The measured OIP3 versus frequency is plotted in Figure 7, and varies between +35 dBm and +37 dBm depending on frequency. The saturated output power of the transmit chain varies between 27 dBm and 28 dBm over the operating band.

CONCLUSIONS

The announcement of the 26 GHz band (24.25 to 27.5 GHz) as the recommended pioneer band for mm-wave 5G in Europe is welcome. However, the availability of some of the key mm-wave components required to allow the development of 5G systems operating in this band is limited. The work reported here has attempted to address this by developing an FEM – comprising LNA, PA and Tx/Rx switch – integrated in a custom laminate SMT package and covering the full 26 GHz 5G band. Low loss transmit and receive filters are integrated into the package body. The transmit filter provides > 20 dB of harmonic rejection after the PA and has a loss of 0.2 dB. The receive filter is a bandpass structure located after the LNA and has an insertion loss of 0.7 dB. Measured performance of the FEM mounted on a representative PCB has been presented and shows good agreement with simulated. Receive path gain is 20 dB with a NF of around 3.5 dB. Transmit path gain is 19 dB with an output referred third order intercept point (OIP3) of +36 dBm.

REFERENCES

[1] Components for mm-wave 5G: https://www.plextekrfi.com/mm-wave/mm-wave-5g/

[2] The EU's Radio Spectrum Policy Group, "Strategic Roadmap Towards 5G for Europe"

[3] Devlin L.M., Dearn A.W. and Pearson G.A., "Low Loss MM-Wave Monolithic SP4Ts", proceedings of the 2001 "Workshop on Design for Broadband Wireless Access", Cambridge, England, 3rd May 2001